Slide 1

Solar Sherlock: Investigating a complex X-class flare using NLFFF modeling

Blake Forland

Mentor: Yingna Su

Slide 2

Introduction

Eruptions on the Sun

CME — Prominence Eruption — Flares

Contribute to space weather

Eruptions are driven by the release of free energy stored in the coronal magnetic field by magnetic reconnection

Studying the topology of coronal magnetic field understand flares

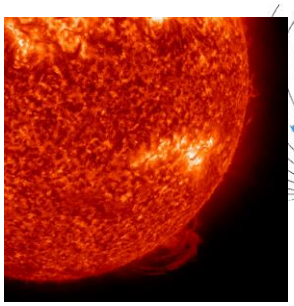

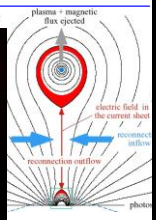

Solar Flare and Prominence Eruption

Slide 3

Modeling

Why do we model solar flares?

The coronal magnetic field is very difficult to measure directly

Allows us to use photospheric magnetic data to describe the corona

Modeling can determine initial parameters for flares

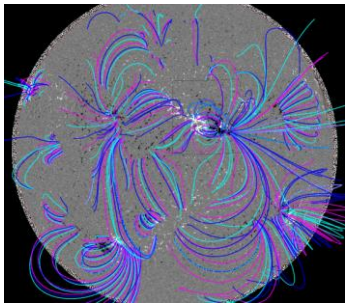

Coronal Potential Field Model

Slide 4

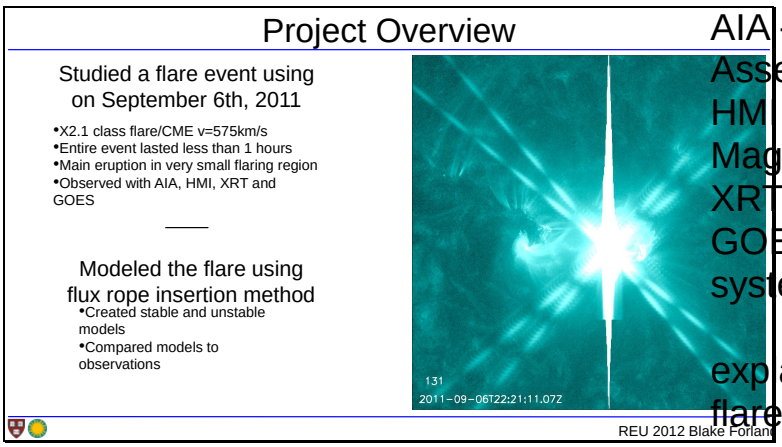

AIA - Atmospheric Imaging Assembly
HMI - Helioseismic and Magnetic Imager
XRT - X-Ray telescope
GOES - Geostationary Satellite system

explain diffraction pattern in flare. Its an artifact of the filters

Slide 5

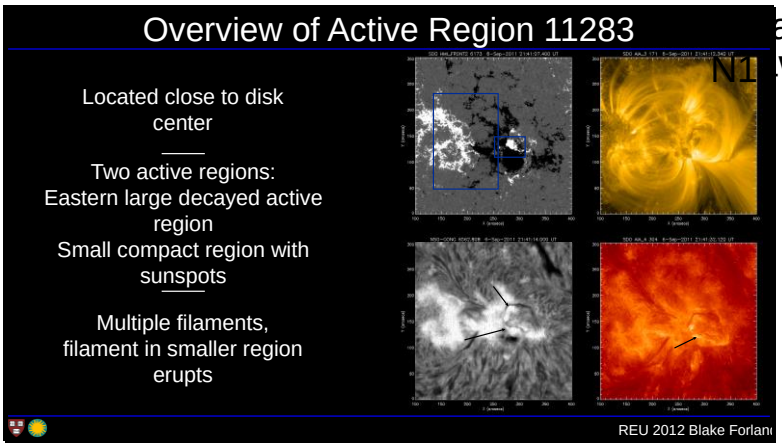

ation:
N1 W16(255",116")

Slide 6

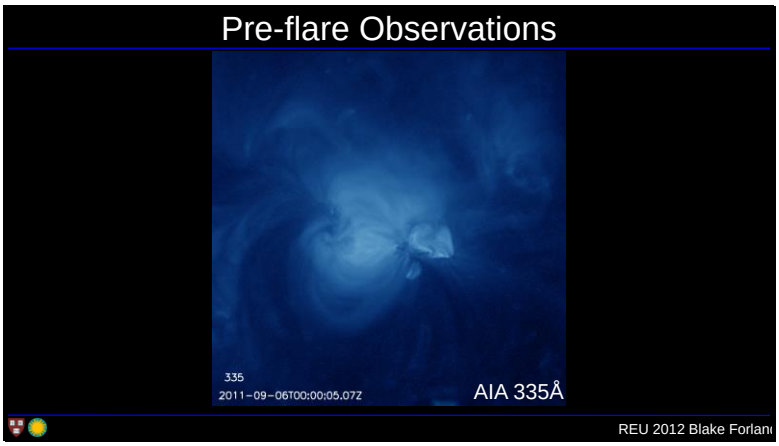

Slide 7

Pre-flare XRT Observations

Many micro-flares can be seen throughout the day before the flare

Smaller region is much more active

Time: 11:18 - 23:59
Cadence: approx. 2 min

Slide 8

Pre-flare HMI Observations

Two interesting observations can be seen in the HMI magnetogram that help to explain how magnetic instability is reached

Flux cancellation — Shear motion

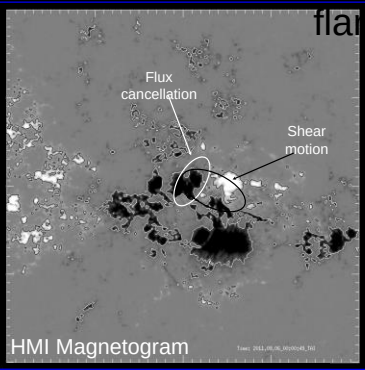

ar motion helps to micro fla es and loss of instability

Slide 9

AIA Flare Observations for 8 Channels

304, 335 and 1600 - Asymmetry in flare ribbons most visible and in 304 the filament eruption that occurs with the flare can be seen

171 - Shows the large scale loops of the active region

94 and 131 - Brightenings can be seen before any other wavelengths

193 and 211 - Overlying magnetic fields can be see being blown away just as flare begins

Brightenings can be seen first in these two wavelengths

193 211 Overlying magnetic fields can be see being blown away in this and in 211

304 - Why does the smaller region flare before the larger region? multiple ribbons

What is the connection to the region to the north west?

1600 - Good for seeing ribbons

Slide 10

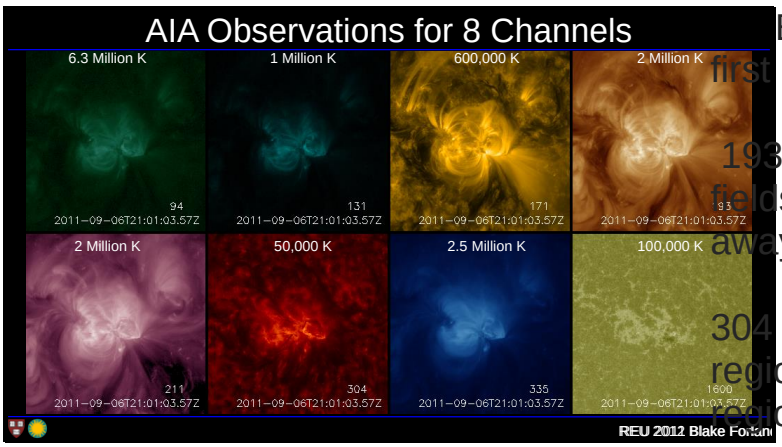

Brightenings can be seen first in these two wavelengths

193 211 Overlying magnetic fields can be see being blown away in this and in 211

304 - Why does the smaller region flare before the larger region?

What is the connection to the region to the north west?

1600 - Good for seeing ribbons

Slide 11

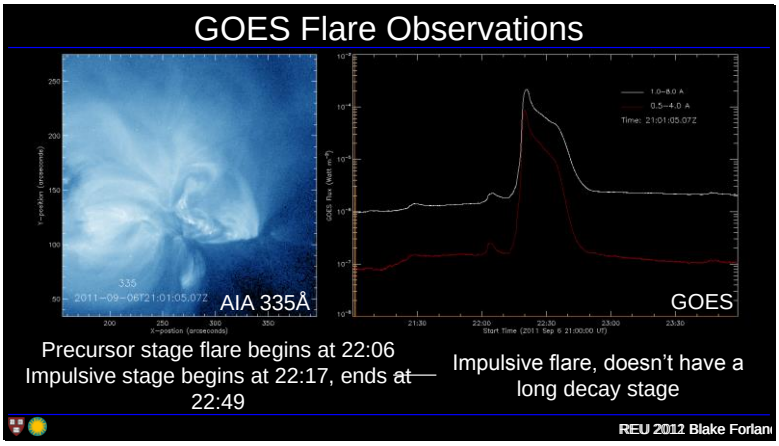

Slide 12

HMI Observations

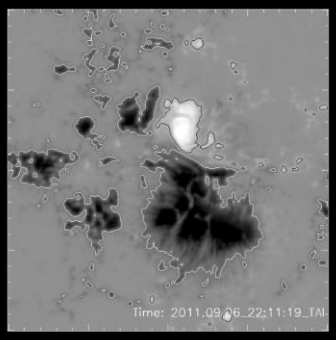

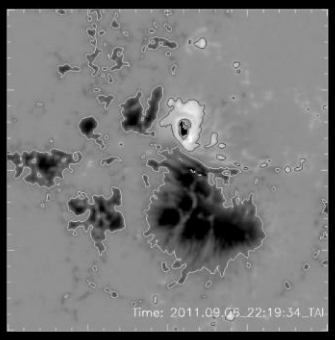

REU 2012 Blake Forland

Slide 13

XRT Flare Observations

Very clear "S" shaped loop

Asymmetry of the time and the intensity of the flare ribbons between the two regions clearly visible

XRT Event Tracking

REU 2012 Blake Forland

r slide One of our attempts is to create a NFFF model for the preflare state

Slide 14

Magnetohydrodynamics

Starting with Maxwell's Equations and Ohm's Law:

$$\nabla \cdot \mathbf{B} = 0 \qquad \nabla \times \mathbf{B} = \mu j$$

$$j = \sigma(\mathbf{E} + \mathbf{v} \times \mathbf{B}) \qquad \nabla \times \mathbf{E} = -\frac{\partial \mathbf{B}}{\partial t}$$

MHD *induction equation:*

$$\frac{\partial \mathbf{B}}{\partial t} = \nabla \times (\mathbf{v} \times \mathbf{B}) + \eta \nabla^2 \mathbf{B}$$

Fluid dynamics mass continuity:

$$\frac{\partial \rho}{\partial t} = -\nabla \cdot (\rho \mathbf{v})$$

Results in the MHD momentum equation:

$$\rho \frac{D\mathbf{v}}{Dt} = -\nabla p + \mathbf{j} \times \mathbf{B} + pg$$

Yeate-thesis2009

Slide 15

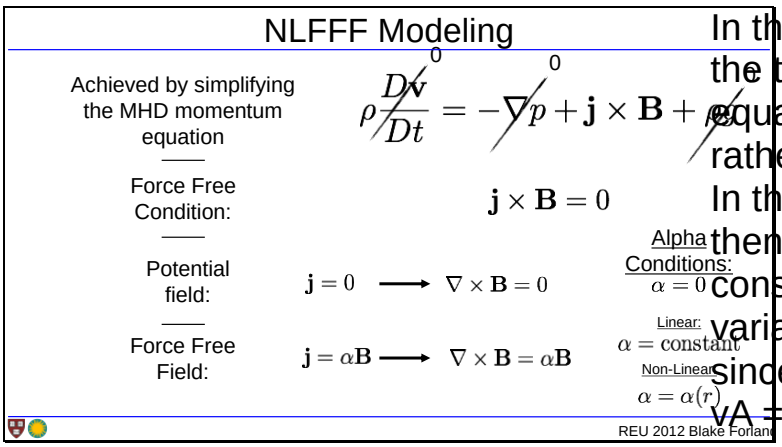

In this thesis we do not solve the time-dependent MHD equations in the corona, but rather we consider equilibria. In the global corona, we may then simplify equation considerably. Firstly, velocity variations may be neglected since $|v| \ll vA$
$vA = |B|/\sqrt{\mu\rho}$ is the Alfve´n speed (approximately 1000 km s−1 in the corona).
Secondly, we may neglect the gravity term as compared to the pressure gradient providing the length scale of interest is less than the pressure scale-height, which is typically of order 105 km in the corona.
Finally, the pressure gradient may be neglected compared to the Lorentz force since, in the corona, $\beta \ll 1$.
The plasma β parameter is the ratio of gas pressure, p, to magnetic pressure, $B2/(2\mu)$.
Thus the magnetic field in the solar corona—except during dynamic events such as coronal mass ejections—may be expected to satisfy
$j \times B = 0$.

Such a field is called force-free, since the Lorentz force vanishes everywhere.

The value of α describes the helical twist of a field line with respect to the potential field $\alpha = 0$

Slide 16

Flux Rope Insertion Method

Select region and create a potential field model

Choose path from observations and insert flux ropes into 3D model

Relax model using magneto-frictional relaxation
- Relaxed State
- Unstable State

Compare models to observations

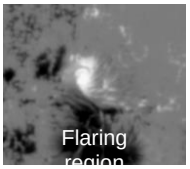

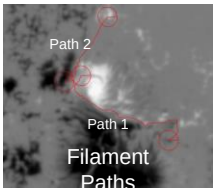

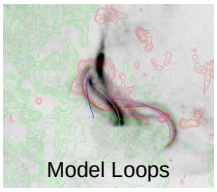

Relaxation doesn't always result in a stable model

Slide 17

Determining Stability

Take multiple cross sections along filament paths

Cross Sections

Arrows show magnetic field direction

Current plot; bright areas means more dense

Stable models remain at the same height throughout 30000 iterations

The flux rope in unstable models is still expanding after 30000 iterations

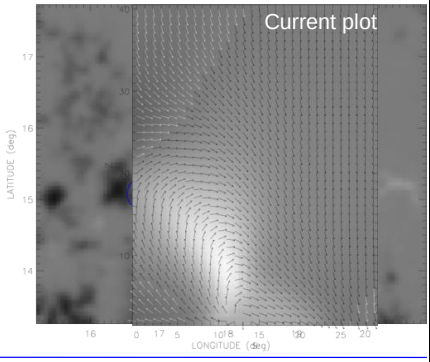

Slide 18

Stability

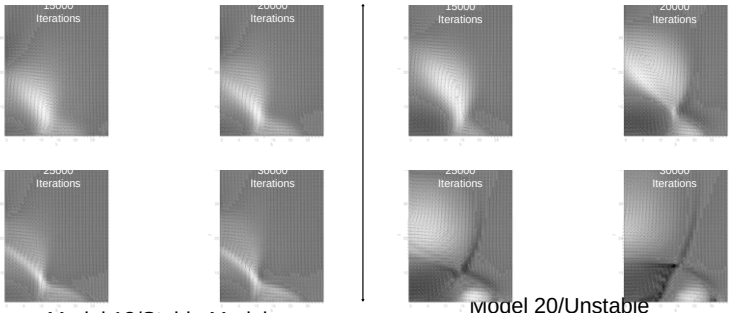

Model 18/Stable Model
Axial Flux: 2e20 Mx
Polodial Flux: 1e20 Mx

Model 20/Unstable Model
Axial Flux: 8e20 Mx
Polodial Flux: 1e20 Mx

REU 2012 Blake Forland

Slide 19

All Completed Model Parameters

Best Fit Model
Path 1: Axial Flux: 4e20 Mx, Polodial Flux: 1e10 Mx cm^{-1}
Path 2: Axial Flux: 2e20 Mx, Polodial Flux: 1e10 Mx cm^{-1}

Unstable Model
Path 1: Axial Flux: 6e20 Mx, Polodial Flux: 1e10 Mx cm^{-1}
Path 2: Axial Flux: 3e20 Mx, Polodial Flux: 1e10 Mx cm^{-1}

Best fit pre-flare model is very close to threshold
Axial flux threshold: 5e20 Mx

	Path 1		Path 2							
Model Number	Axial Flux (10^{20} Mx)	Poloidal Flux (10^{10} Mx cm^{-1})	Axial Flux (10^{20} Mx)	Poloidal Flux (10^{10} Mx cm^{-1})	E_{free} (10^{31} Erg)	$E_{free}/E_{potential}$ %	Stable	ADa ± 0.2 (10−3 Rsun) Loop 1	Loop 2	Loop 3
6	2	0	0	0	2.54	5.1	Y	2.5	1.1	5.6
7	3	0	0	0	4.03	8.1	Y	1.5	0.4	2.5
3	4	0	0	0	4.03	8.1	Y	1.6	0.4	2.5
11	4	1	0	0	4.20	8.5	Y	1.5	0.4	2.4
12	4	10	0	0	4.67	9.4	Y	1.3	0.4	2.6
15	4	30	0	0	3.30	6.7	Y	1.8	0.5	3.7
16	4	50	0	0	6.83	13.8	N	0.4	0.4	5.3
17	4	1	1	1	3.57	7.2	Y	1.7	0.5	1.9
18	**4**	**1**	**2**	**1**	**3.61**	**7.3**	**Y**	**1.7**	**0.5**	**1.8**
19	4	1	3	1	3.64	7.3	Y	1.7	0.5	1.8
8	5	0	0	0	5.00	10.1	Y	1.7	0.5	2.6
13	5	1	0	0	5.07	10.2	N	1.6	0.5	2.5
14	5	10	0	0	5.64	11.4	Y	1.4	0.6	2.6
9	6	0	0	0	5.31	10.7	N	2.1	0.3	4.2
20	6	0	3	1	4.62	9.3	N	2.1	0.3	4.2
10	7	0	0	0	5.31	10.7	N	2.5	0.4	5.1
4	8	0	0	0	5.41	10.9	N	2.7	0.6	5.5

REU 2012 Blake Forland

Slide 20

Best Fit Pre-Flare Model

Best Fit Model
Path 1: Axial Flux: 4e20 Mx, Polodial Flux: 1e10 Mx cm^{-1}
Path 2: Axial Flux: 2e20 Mx, Polodial Flux: 1e10 Mx cm^{-1}

Free energy: 3.61e31 Erg

Potential energy: 4.95e32 Erg

Percentage of potential energy: 7.3 %

Model also matches large scale field lines

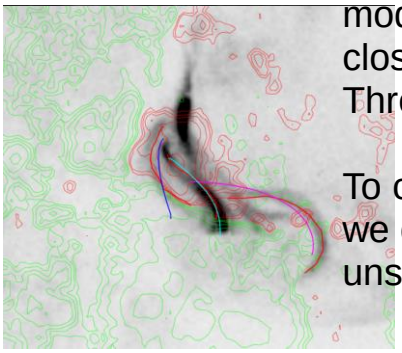

REU 2012 Blake Forland

We determine the best fit model in order to find out how close it is to unstable. Threshold

To compare with flare ribbons we created QSL maps of unstable model

Slide 21

Quasi-separatrix Layer Map

QSL map shows the values of the squashing factor Q

Blue: Low Q

and Yellow: High Q

Green: Outside computational domain

Region where magnetic field line linkage changes drastically

Yellow regions can point to sites of magnetic reconnection

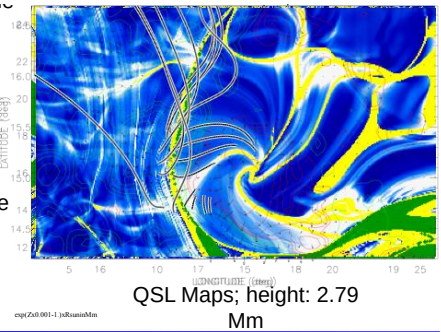

QSL Maps; height: 2.79 Mm

Slide 22

Potential QSL map vs. Unstable QSL map

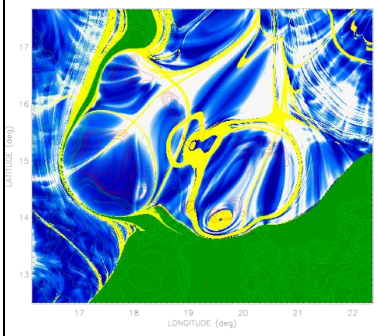

Potential Field Model

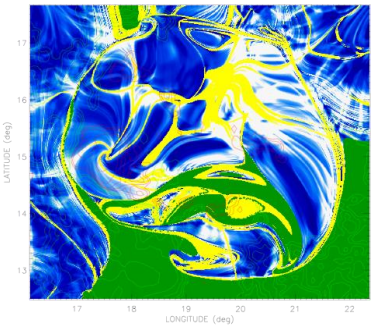

Model 9/Unstable Model

Slide 23

Observations vs. Unstable QSL map

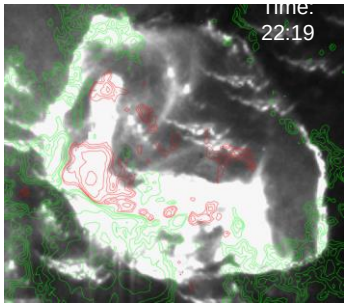

AIA 335Å

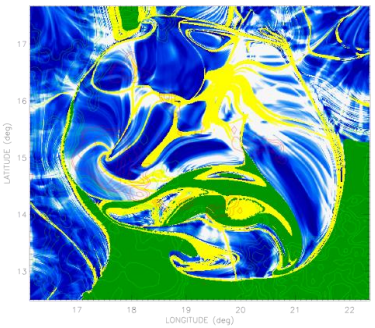

Model 9/Unstable Model

Slide 24

Interpreting Multiple Flare Ribbons

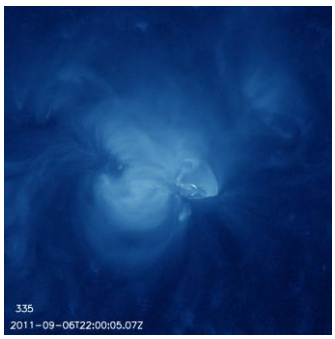

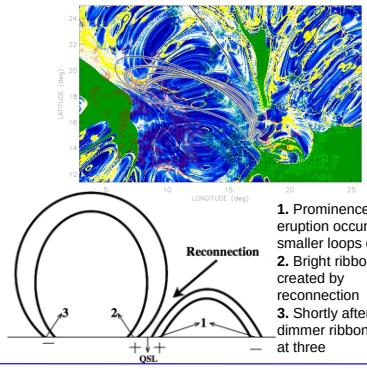

1. Prominence eruption occurs and smaller loops expand
2. Bright ribbons created by reconnection
3. Shortly after dimmer ribbon is seen at three

Slide 25

Reconnection Magnetic Field Strength

Unstable Model

Path 1 Cross section

X - Site of reconnection, height: 6.26 Mm

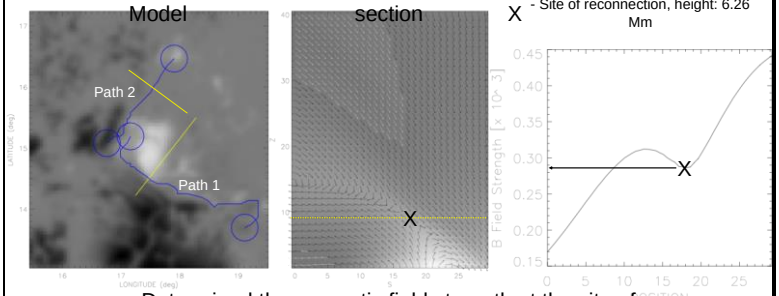

Determined the magnetic field strength at the site of reconnection for Path 1: 286 G and estimated the strength along Path 2: 30 G.

Slide 26

Conclusions

Studied an impulsive X2.1 class flare. The flare was accompanied by a filament eruption and during the flaring interesting asymmetric flare ribbons were observed in difference parts of the active region.

Axial flux of the best fit pre-flare model is close to threshold instability which suggests flare my be triggered by loss of equilibrium due to build up of axial flux driven by shear motion.

Best fit pre-flare model had free energy 3.61e31 Erg which is much smaller than expected energy release during X class flares

Regions at strong QSLs were consistent with observed ribbons and field line linkage at QSLs helped to understand multiple asymmetric flare ribbons

Measured magnetic field strength of 286 G for flaring near region reconnection site; Estimated 30G for path 2

Slide 27

Acknowledgments

Mentor: Yingna Su

Aad van Ballegooijen

Kathy Reeves

Jonathan Sattelberger

Harvard-Smithsonian Center for Astrophysics

National Science Foundation

Harvard University

Slide 28

Questions?